

6 and 7 is small relative to the first term so that

$$\gamma_+ \approx S_1 = \frac{(k_{12} + k_{13})K_{a2}[\text{Ni}^{2+}]}{(K_{a2} + [\text{H}^+])} + \frac{k_{13}K_{a2}[\text{H}^+]}{K_C(K_{a''} + [\text{H}^+])} \quad (8)$$

$$\gamma_- \approx S_2 = \frac{k_{12}K_{a2}K_{a'}}{K_S(K_{a'} + [\text{H}^+])} + k_{23} \left(\frac{K_{a'}}{(K_{a'} + [\text{H}^+])} + \frac{K_S[\text{H}^+]}{K_C(K_{a''} + [\text{H}^+])} \right) \quad (9)$$

Since $K_{a2} = 1.5 \times 10^{-10} \ll [\text{H}^+]$, inspection of eq 8 shows that γ_+ will have a dependence on $[\text{Ni}^{2+}]$ and $[\text{H}^+]$ consistent with eq 4 if $K_{a''} \ll [\text{H}^+]$ and K_C is large enough or k_{13} is small enough so that the last term in eq 8 is not dominant. On the other hand, eq 9 predicts that γ_- should be independent of $[\text{Ni}^{2+}]$ because the last term in eq 7 disappears in the first-order approximation used to obtain eq 9. The magnitude of γ_- depends directly on k_{12} and k_{23} , but the former may be established by γ_+ so that at least an upper limit on the value of k_{23} is determined from γ_- . In addition, γ_- will not show much pH dependence if $K_{a'} > [\text{H}^+]$ and $K_{a''} \ll [\text{H}^+]$. It is noteworthy that if K_C is decreased in eq 8, then k_{13} will decrease to maintain the magnitude of the last term and k_{12} will increase to keep the first term constant. But the latter increase may be limited by the magnitude of γ_- . It should be apparent that it will be possible to evaluate $k_{12} + k_{13}$ from eq 8, but the separation of the terms will depend on K_C in eq 8 and K_S in eq 9.

Qualitatively k_1 (γ_+) varies with $[\text{Ni}^{2+}]$ and pH as predicted by eq 8 and k_2 (γ_-) is relatively independent of these variables as required by eq 9. The values of k_1 (γ_+) and k_2 (γ_-) have been fitted simultaneously by a nonlinear least-squares method to eq 5 while various constraints were imposed on the equilibrium constants, as indicated by the pH titration results. The experimental and calculated results are compared in Table II. As expected from the above discussion, the value of $k_{12} + k_{13}$ is well-defined at $(3.5 \pm 1.1) \times 10^5 \text{ M}^{-1} \text{ s}^{-1}$. A "best fit" is obtained with $K_S + (K_C/K_{a''}) = 6 \times 10^{-6}$ and $K_S = 2.5 \times 10^{-6}$, which gives $k_{12} = (1.9 \pm 0.7) \times 10^5 \text{ M}^{-1} \text{ s}^{-1}$ and $k_{13} = (1.4 \pm 0.7) \times 10^5 \text{ M}^{-1}$

s^{-1} , while k_{23} is undefined at $0.28 \pm 4.8 \text{ s}^{-1}$. The latter value indicates that the intramolecular rearrangement path is not significant in the linkage isomerism process in this system. The values of k_{12} and k_{13} are similar, as expected for a dissociative ion pair substitution on $\text{Ni}(\text{OH}_2)_6^{2+}$, and their magnitude is consistent with that expected for reaction of a dianion.⁸

In summary, it has been found that the complexing of $\text{Ni}(\text{OH}_2)_6^{2+}$ by 2,3-dihydroxybenzoate is not a simple kinetic process and that the complexity can be accounted for by the formation of salicylate and catecholate linkage isomers. In this labile system, the linkage isomerism proceeds predominantly by dissociation and recomplexation rather than by an intramolecular rearrangement.

Experimental Section

Materials. All solutions for kinetic and equilibrium studies were prepared in deionized water distilled from alkaline permanganate in an all-glass apparatus. The nickel(II) solutions were prepared by dissolving reagent grade nickel nitrate (Fisher) in water and standardized by EDTA titration.

The ligand solutions were made by dissolving weighed amounts of 2,3-dihydroxybenzoic acid (Aldrich) in water and diluting to volume. These solutions were prepared fresh daily and stored under argon. When required, the solutions contained PIPES buffer (Sigma) and the pH was adjusted to the desired value before dilution to known volume. All solutions contained enough NaNO_3 to give an ionic strength of 0.30 M.

For the titration studies, solutions containing $9.62 \times 10^{-4} \text{ M}$ DHB and various concentrations of nickel(II) (0.010–0.050 M) in 0.30 M NaNO_3 were titrated with 0.0102 M NaOH. The pH meter was calibrated to give $[\text{H}^+]$ by titrating 0.0100 M HCl with the same NaOH between pH 2 and 5.5.

Instrumentation. Preliminary spectrophotometric observations were done on Cary 219 and Hewlett-Packard 8451 spectrophotometers. The pH was determined on a Corning 124 pH meter standardized with appropriate buffers. The stopped-flow observations were done on an Aminco-Morrow stopped-flow system. The rate constants have been determined from the average of five to seven runs with the same solutions under a particular set of conditions.

Acknowledgment. We thank the Natural Sciences and Engineering Research Council of Canada for financial support, and L.C. thanks the Coordination Chemistry Institute of Nanjing University for granting a study leave to do this work.

Contribution from the Department of Chemistry,
Chung-Yuan Christian University, Chungli 32023, Taiwan, Republic of China

Characterization of Pentacyanoferrate(II) and -(III) Complexes of Adenosine and Related Aminopyridine Ligands

C. H. Hung, H. Y. Huang, J. Y. Liao, and A. Yeh*

Received January 5, 1989

A series of $\text{Fe}(\text{CN})_5\text{L}^{3-}$ complexes, where L = adenosine, 1-methyladenosine, tubercidin, and 2- and 3-aminopyridines, were prepared and characterized in aqueous solution. A metal to ligand charge-transfer transition was observed for complexes of adenosine (337 nm), tubercidin (340 nm), 2-aminopyridine (345 nm), and 3-aminopyridine (362 nm). Their corresponding Fe(III) complexes also display a ligand to metal charge-transfer absorption at 570 (adenosine), 635 (tubercidin), 655 (2-aminopyridine) and 695 nm (3-aminopyridine). The 1-methyladenosine complex of pentacyanoferrate(II) exhibits a band maximum at 375 nm, which is similar to that of imidazole complex. The rate constants of formation and dissociation were measured, and the k_f and k_d values (25 °C, $\mu = 0.10 \text{ M}$ (LiClO_4), pH = 8) are $269 \text{ M}^{-1} \text{ s}^{-1}$ and $9.70 \times 10^{-2} \text{ s}^{-1}$ (adenosine), $257 \text{ M}^{-1} \text{ s}^{-1}$ and 0.612 s^{-1} (1-methyladenosine), $70.4 \text{ M}^{-1} \text{ s}^{-1}$ and 0.596 s^{-1} (tubercidin), $401 \text{ M}^{-1} \text{ s}^{-1}$ and 0.585 s^{-1} (2-aminopyridine), and $310 \text{ M}^{-1} \text{ s}^{-1}$ and $1.84 \times 10^{-3} \text{ s}^{-1}$ (3-aminopyridine). Cyclic voltammetry of the complexes under study has shown that the oxidation is a one-electron reversible process with $E_{1/2}$ values of 0.49 (adenosine), 0.44 (tubercidin), 0.41 (2-aminopyridine), and 0.43 V (3-aminopyridine) vs. NHE at 25 °C, $\mu = 0.10 \text{ M}$ (LiClO_4), and pH = 8 (Tris). Both spectral and electrochemical results suggest that the coordination site of both $\text{Fe}(\text{CN})_5\text{ado}^{3-}$ and $\text{Fe}(\text{CN})_5\text{ado}^{2-}$ complexes is at N-1 of the nucleic acid and there is no linkage isomerization from N-1 to the exocyclic nitrogen when the metal center is oxidized from Fe(II) to Fe(III).

The complexes of pentaammineruthenium(II) and -(III) with various nucleic acids have been well characterized during the past decade.¹⁻⁵ One of the advantages of using the ruthenium ammine

metal center is its substitution inertia in both the 2+ and 3+ oxidation states, which may simplify the experimental results and provide a way to systematically study the effect of the metal ion

(1) Clarke, M. J.; Taube, H. *J. Am. Chem. Soc.* **1974**, *96*, 5413.
(2) Clarke, M. J.; Taube, H. *J. Am. Chem. Soc.* **1975**, *97*, 1397.
(3) Clarke, M. J. *Inorg. Chem.* **1977**, *16*, 739.

(4) Clarke, M. J. *J. Am. Chem. Soc.* **1978**, *100*, 5068.
(5) Brown, G. M.; Sutton, J. E.; Taube, H. *J. Am. Chem. Soc.* **1978**, *100*, 2767.

on a ligand moiety. The study has recently been further extended to the investigations of the complexes formed by the interaction of Ru(NH₃)₅OH₂²⁺ with DNA.⁶⁻⁸

Studies of pentacyanoferrate(II)⁹ and -(III)¹⁰ complexes have shown strong similarities in optical and chemical properties of these complexes with those of the corresponding pentaammineruthenium complexes. Thus it is worthwhile to extend the study to the purine base complexes of the Fe(CN)₅L^{3-/2-} moiety. In this paper we report the kinetics and spectroscopic and electrochemical properties of the adenosine complex of pentacyanoferrate(II) and -(III) in aqueous solution. In order to understand the preferred coordination site of the metal center and the effect of the amino group in the pyrimidine ring on the properties of the complex, studies on the Fe(CN)₅L^{3-/2-} complexes with L = 1-methyladenosine, tubercidin, and 2-, 3-, 4-aminopyridines have also been carried out.

Experimental Section

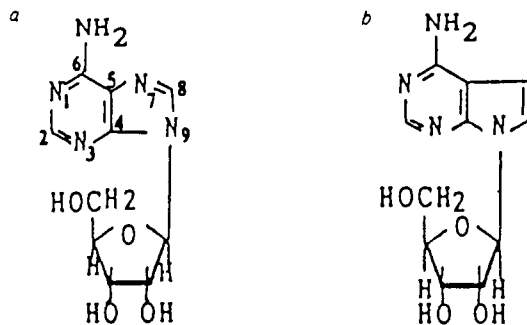
Materials. 1-Methyladenosine was prepared by methylation of adenosine (Sigma) with methyl iodide according to the literature method.¹¹ The solutions of pentacyanoferrate(II) complexes under study were prepared by the dissolution of Na₃Fe(CN)₅NH₃·3H₂O^{12,13} in solutions containing large excesses of ligands. The corresponding Fe(III) complexes were obtained by the oxidation of the solutions of the Fe(II) complexes with 1 equiv of cerium(IV). The cerium(IV) solution was prepared by dissolving (NH₄)₂Ce(NO₃)₆ (RDH) in 1 N HClO₄. Its concentration was standardized by ferrous sulfate, with ferroin used as an indicator. Both Fe(CN)₅ado²⁻ and Fe(CN)₅-2-Ampy²⁻ were also isolated as solid salts. For the adenosine complex, 0.1 g of Na₃[Fe(CN)₅NH₃]₃H₂O was added to a solution containing 0.27 g of adenosine in 20 mL of water. After the mixture was bubbled with nitrogen in the absence of light for 15 min, the resulting solution was oxidized with bromine vapor until the solution turned from yellow to purplish blue. A saturated solution of MnCl₂·4H₂O (RDH) was then added dropwise until a permanent turbidity was observed. After the mixture was cooled at 5 °C for 2 h, the precipitate was collected by filtration and was washed with ethanol and ether. Anal. Calcd for Mn[Fe(CN)₅C₁₀H₁₃N₅O₄]₃H₂O: C, 32.0; N, 24.9; H, 3.41. Found: C, 31.1; N, 24.4; H, 3.94. Copper (2-aminopyridine)pentacyanoferrate(III) was prepared by adding 0.2 g of Na₃[Fe(CN)₅NH₃]₃H₂O to 10 mL of water containing 2.5 g of 2-aminopyridine, and the reaction was allowed to proceed in the dark and under a nitrogen atmosphere for 15 min. Bromine vapor was then introduced to the solution until the color changed from yellow to blue. At this point a saturated solution of CuSO₄·5H₂O (RDH) was added dropwise until a precipitate began to form. After the mixture was cooled in an ice bath for 2 h, the product was filtered out, washed with ethanol and ether, and then dried in a vacuum desiccator overnight. Anal. Calcd for Cu[Fe(CN)₅C₅H₆N₂]₃H₂O: C, 30.2; N, 24.7; H, 3.04. Found: C, 30.7; N, 24.8; H, 2.82. The ν(CN) of the infrared spectra at about 2120 cm⁻¹ for both complexes further confirms the formation of Fe(III) complexes.¹⁴

Tubercidin was purchased from Wako Pure Chemical Industries and was used as received. All solutions were prepared from house-line distilled water, which was further purified by passing it through a Kintech Model DI-S4 Ultra Pure Water system. All other chemicals were reagent grade and were used without further purification.

Kinetic Measurements. Rates of formation of Fe(CN)₅L³⁻ (L = adenosine, 1-methyladenosine, tubercidin, and 2-, 3-, and 4-aminopyridines) complexes were measured spectrophotometrically by mixing the freshly prepared Fe(CN)₅OH₂³⁻ solution with excess ligands on a Photal RA-401 stopped-flow apparatus (Union Giken), which was interfaced with a NEC 9801VX microcomputer for data acquisition and analysis. The measurements were carried out by following the absor-

Table I. Absorption Maxima for the Pentacyanoferrate(II) and -(III) Complexes

ligand	Fe(CN) ₅ L ³⁻	Fe(CN) ₅ L ²⁻
	λ _{max} , nm (10 ³ ε _{max})	λ _{max} , nm (10 ³ ε _{max})
adenosine ^a	337 (1.34), 400 (0.70) ^c	364 (0.85), 390 (0.83), 570 (0.35)
1-methyladenosine	375 (1.61) ^c	400 (1.87)
tubercidin ^b	340 (1.83), 404 (1.16)	400 (0.99), 635 (0.23)
2-aminopyridine	345 (1.80), 398 (1.02)	655 (1.56)
3-aminopyridine	362 (4.42)	695 (1.01)
4-aminopyridine	320 (4.37), 398 (0.70)	560 (2.75)
	320 (4.4) ^d	560 (2.8) ^d
imidazole	383 (0.43) ^e	356 (0.981), 403 (1.18), 475 (0.376) ^f
aniline	415 (0.517)	
pyridine	362 (3.72) ^g	368 (0.8), 414 (1.1) ^h
pyrimidine	410 (3.1) ⁱ	



^a pH = 2–8. ^dReference 15. ^eReference 16. ^fReference 10. ^gReference 9. ^hReference 17. ⁱReference 21.

ance increase at band maxima of the complexes. Fe(CN)₅OH₂³⁻ solution was prepared by the aqution of Fe(CN)₅NH₃³⁻¹⁵ at 25 °C for approximately 5 min in the absence of light prior to each run. The kinetic measurements were performed within 10 min after the preparation of the solution. The observation of a constant A_∞ at the end of the reaction in each kinetic run indicates that there is no dimerization of Fe(CN)₅OH₂³⁻ during the complex formation. Rates of dissociation of the complexes were measured by adding an excess of pyrazine to a solution of the complex and following the formation of the pyrazine complex at its maximum wavelength of absorption (λ_{max} = 452 nm).⁹ The measurements were performed either on a Specord M40 spectrophotometer (L = 3- and 4-aminopyridines) or on a stopped-flow spectrophotometer (L = adenosine, 1-methyladenosine, and 2-aminopyridine), depending on the rate of the reaction. The observed rate constants were obtained from the slopes of the linear least-squares fits of ln(A_∞ - A_t) vs time plots. Temperatures of the experiments were controlled by a Hotech 631-D temperature bath.

Electrochemical Measurements. All electrochemical measurements were performed on a PAR Model 363 potentiostat and Model 175 universal programmer system. Cyclic voltammograms were obtained on a Rikadenki Model RW-101 X-Y recorder. A conventional two-compartment electrochemical cell separated by a glass frit of medium porosity was used for the measurements. The working electrode was either carbon paste or a platinum wire. The platinum wire was also used as the counter electrode, and a saturated calomel electrode, as the referenced electrode. The complex solution was kept at ~1 × 10⁻³ M, and the ionic strength was maintained at μ = 0.10 M (LiClO₄).

Results and Discussion

Absorption Spectra. The properties of the UV-visible spectra of the pentacyanoferrate(II) and -(III) complexes are summarized in Table I. Two absorption bands were observed for the Fe(II) complexes of adenosine and some other ligands. The absorption shoulders around 400 nm were found to be independent of the ligand concentration and were present even in the absence of the ligand, as shown in Figure 1. Therefore we may assign these bands as the d-d transition from the ¹A₁ ground state to the ¹E(1) excited state due to the pentacyanoferrate metal center.¹⁷ The

- Clarke, M. J.; Buchbinder, M. *Inorg. Chim. Acta* **1977**, *27*, 287.
- Clarke, M. J.; Jansen, B.; Marx, K. A.; Kruger, R. *Inorg. Chim. Acta* **1986**, *124*, 13.
- Wielopolski, L.; Zhang, R.; Clarke, M. J.; Cohn, S. H. *Biol. Trace Elem. Res.* **1987**, *13*, 283.
- Toma, H. E.; Malin, J. M. *Inorg. Chem.* **1973**, *12*, 1039.
- Johnson, C. R.; Henderson, W. W.; Shepherd, R. E. *Inorg. Chem.* **1984**, *23*, 2754.
- Jones, J. W.; Robins, R. K. *J. Am. Chem. Soc.* **1963**, *85*, 193.
- Brauer, G. *Handbook of Preparative Inorganic Chemistry*, 2nd ed.; Academic Press: New York, 1965; p 1511.
- Jwo, J. J.; Haim, A. *J. Am. Chem. Soc.* **1976**, *98*, 1172.
- Dows, D. A.; Wilmarth, W. K.; Haim, A. *J. Inorg. Nucl. Chem.* **1961**, *21*, 33.

- Szecsny, A. P.; Miller, S. S.; Haim, A. *Inorg. Chim. Acta* **1978**, *28*, 189.
- Hrepic, N. V.; Malin, J. M. *Inorg. Chem.* **1979**, *18*, 409.
- Toma, H. E.; Martins, J. M.; Giesbrecht, E. *J. Chem. Soc., Dalton Trans.* **1978**, 1610.

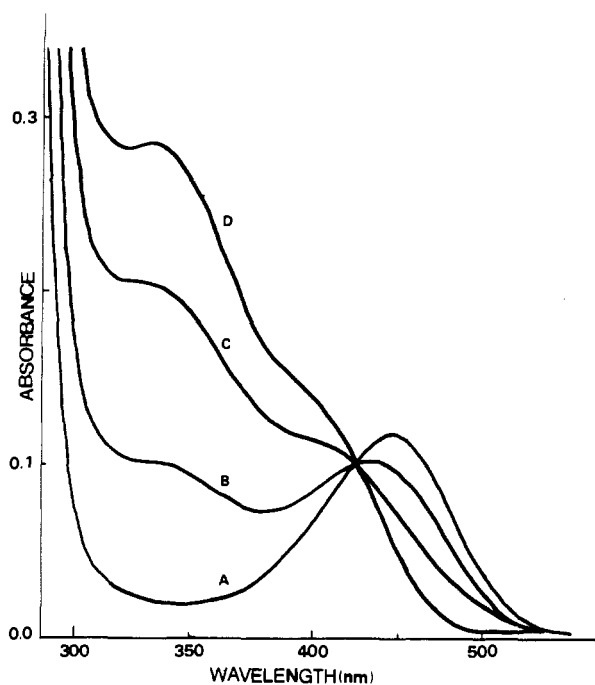


Figure 1. Absorption spectra of $\text{Fe}(\text{CN})_5\text{ado}^{3-}$ at different adenosine concentrations ($[\text{Fe}(\text{CN})_5\text{OH}_2^{3-}] = 2.01 \times 10^{-4} \text{ M}$ (25°C , 0.10 M LiClO_4): (A) absence of adenosine; (B) $[\text{ado}] = 2.21 \times 10^{-4} \text{ M}$; (C) $[\text{ado}] = 1.01 \times 10^{-3} \text{ M}$; (D) $[\text{ado}] = 9.91 \times 10^{-3} \text{ M}$.

intense high-energy bands in the 320–360-nm region are characteristic of the $\text{Fe}(\text{II})$ –aromatic N-heterocyclic complexes⁹ and can be interpreted as due to the $d_{\pi} \rightarrow \pi^*$ charge-transfer absorptions. All $\text{Fe}(\text{CN})_5\text{L}^{2-}$ complexes with ligands containing an amino group showed an absorption in the low-energy region of their spectra in addition to the well-defined bands characteristic of the $\text{CN}^- \rightarrow \text{Fe}(\text{III})$ (350–360 nm) and the ligand field splittings (390–400 nm).^{10,18} The absorption apparently arises from a ligand to metal charge-transfer (LMCT) transition.

One of the difficulties in the investigations of metal ion interactions with nucleic acids is the determination of the metal binding site. Previous work with purine complexes of pentaammineruthenium indicated that the charge-transfer transition demonstrated by these complexes can be of assistance in assigning the binding site.^{1–4} For the adenosine ligand, there are three possible positions available for metal binding. Among them, N-3 is sterically hindered by the ribose from the attack of a metal ion, leaving only the N-1 and the N-7 sites.⁴ The similarity of absorption spectra of the $\text{Fe}(\text{CN})_5\text{ado}^{3-}$ (ado = adenosine) complex with those of the corresponding 2-, 3-, and 4-aminopyridine complexes suggests that the $\text{Fe}(\text{II})$ coordination to the adenosine is through the N-1 position of the ligand. The absorption at higher energy than that of the other analogous pyridine complexes has been interpreted^{16,19} as a result of the coupling of the lone-pair electrons on the amine nitrogen with the π^* levels of the aromatic ring. The spectral results for the 1-methyladenosine (1-MeAdo) and tubercidin (tub) complexes further confirm our assignment. Both 1-methyladenosine and tubercidin have only one site permitted for metal interaction, namely N-7 and N-1, respectively. Taking the absorption spectra of $\text{Fe}(\text{II})$ –1-MeAdo (375 nm) and $\text{Fe}(\text{II})$ –tub (340 nm) as representing the LMCT band of the $\text{Fe}(\text{II})$ –ado complex binding on N-7 and N-1, respectively, the observed absorption at 337 nm for the $\text{Fe}(\text{CN})_5\text{ado}^{3-}$ complex can therefore be taken to indicate that the binding site is through N-1. The absorption of the $\text{Fe}(\text{CN})_5$ –1-MeAdo³⁻ complex is similar to that of the $\text{Fe}(\text{CN})_5$ –im³⁻ (im = imidazole) complex, as is expected. An alternative binding site of the adenosine would be the exocyclic amine nitrogen of the pyrimidine ring. However, this possibility can be ruled out by comparing the absorption spectrum of the

Table II. Observed Rate Constants of Formation of Pentacyanoferrate(II) Complexes^a

ligand	$10^4[\text{ligand}]$, M	k_{obs} , s^{-1}	ligand	$10^4[\text{ligand}]$, M	k_{obs} , s^{-1}
adenosine	8.10	0.261	2-amino-pyridine	9.24	0.900
	12.1	0.332		19.1	1.33
	20.2	0.451		41.2	2.18
	25.0	0.537	60.0	2.95	
	40.0	0.991	3-amino-pyridine	2.90	0.0974
80.2	2.04	5.13		0.167	
1-methyl-adenosine	161	4.43	6.93	0.219	
	2.01	0.761	9.48	0.282	
	4.00	0.798	4-amino-pyridine	2.54	0.106
	6.00	0.853		5.02	0.214
tubercidin	7.99	0.914	10.0	0.416	
	4.13	0.476			
	8.10	0.522			
	15.4	0.612			
	20.9	0.679			

^a $[\text{Fe}(\text{CN})_5\text{OH}_2^{3-}] = (1-4) \times 10^{-5} \text{ M}$, $T = 25^\circ \text{C}$, $\mu = 0.10 \text{ N}$ (LiClO_4), $\text{pH} = 8$ (Tris).

Table III. Rate Constants of Formation and Dissociation of Pentacyanoferrate(II) Complexes^a

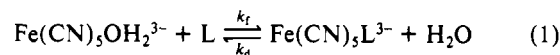
ligand	k_f , $\text{M}^{-1} \text{s}^{-1}$	k_d , s^{-1}	K_{II} , M^{-1}	K_{III} , M^{-1}
adenosine	269 ± 9	$(9.70 \pm 0.04) \times 10^{-2}$	2.77×10^3	56
1-methyl-adenosine	257 ± 19	0.612 ± 0.001	4.20×10^2	3.0×10^3
tubercidin	121 ± 1	0.703 ± 0.011^e	2.85×10^2	40
2-amino-pyridine	401 ± 5	0.452 ± 0.002	6.85×10^2	3.1×10^2
3-amino-pyridine	310 ± 10	0.543 ± 0.020^e	$(1.84 \pm 0.11) \times 10^{-3}$	1.68×10^5
4-amino-pyridine	419 ± 4	$(3.57 \pm 0.06) \times 10^{-3}$	1.17×10^5	1.20×10^6
imidazole	432 ± 10^f	$(2.5 \pm 0.1) \times 10^{-3}$	1.73×10^5	
	240^g	1.33×10^{-3}	1.8×10^5	$8.3 \times 10^5^h$

^a $T = 25^\circ \text{C}$, $\mu = 0.10 \text{ M}$ (LiClO_4), $\text{pH} = 8$ (Tris). ^b [pyrazine] = 0.1–1 M, $[\text{Fe}(\text{CN})_5\text{L}^{3-}] = (1-2) \times 10^{-4} \text{ M}$. ^c Calculated from k_f/k_d . ^d Calculated from eq 2. ^e Obtained from the intercept of the k_{obs} vs [L] plot. ^f Reference 15. ^g Reference 16. ^h Reference 22.

adenosine complex with that of aniline complex. The spectrum of $\text{Fe}(\text{CN})_5\text{an}^{3-}$ (an = aniline) shows $\lambda_{\text{max}} = 415 \text{ nm}$ ($\epsilon_{\text{max}} = 507 \text{ M}^{-1} \text{ cm}^{-1}$), indicating that the back-bonding stabilization is rather weak for the exocyclic amine nitrogen and no LMCT band will be observed when the metal center binds through this position.

The absorption spectrum of $\text{Fe}(\text{CN})_5\text{ado}^{2-}$ also supports the N-1 assignment of the structure. When the $\text{Fe}(\text{II})$ –ado complex is oxidized to the $\text{Fe}(\text{III})$ complex, the solution turns blue immediately, and an absorption at $\lambda_{\text{max}} = 570 \text{ nm}$ is formed. Similar observations are obtained for the $\text{Fe}(\text{III})$ –tub and other $\text{Fe}(\text{III})$ complexes of pyridine-like ligands with an exocyclic amine group, but not for the $\text{Fe}(\text{III})$ –1-MeAdo complex. This low-energy absorption has been assigned as a LMCT transition originating in the HOMO of the ligand containing the lone-pair electrons of the amine nitrogen.^{16,19}

Kinetics of Formation and Dissociation of Pentacyanoferrate(II) Complexes. The rate constants of formation and dissociation reactions according to eq 1 were measured spectrophotometrically.



The formation reactions were found to be first order in $\text{Fe}(\text{CN})_5\text{OH}_2^{3-}$ and first order in ligands. The observed rate constants of formation at various concentrations of ligands are given in Table II. The second-order rate constants as obtained from the slopes of the k_{obs} vs [L] plots are listed in column 2 of Table III. Plots of this kind for adenosine and 2-aminopyridine complexes are shown in Figure 2. As indicated in Table III, the k_f values are independent of the ligand properties and agree with those expected for neutral ligands reacting with $\text{Fe}(\text{CN})_5\text{OH}_2^{3-}$.^{15–17,20,21}

(18) Toma, H. E.; Malin, J. M. *J. Am. Chem. Soc.* **1975**, *97*, 288.

(19) Sutton, J. E.; Taube, H. *Inorg. Chem.* **1981**, *20*, 4021.

(20) Toma, H. E.; Malin, J. M. *Inorg. Chem.* **1973**, *12*, 2080.

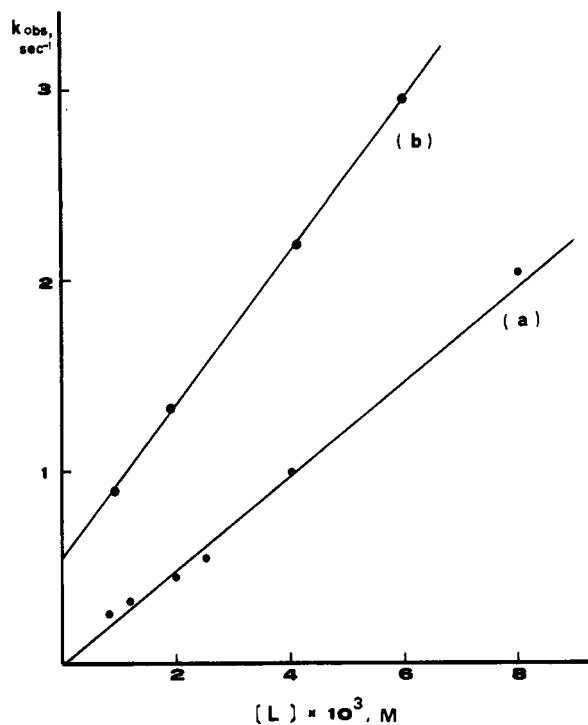


Figure 2. k_{obs} vs $[L]$ plots (pH = 8, $\mu = 0.10$ M (LiClO₄), $T = 25$ °C): (a) Fe(CN)₅sado³⁻; (b) Fe(CN)₅-2-Ampy³⁻.

Table IV. Temperature Dependence of Formation and Dissociation for (Adenosine)pentacyanoferrate(II) Complexes^a

T , °C	$10^{-2}k_f$, M ⁻¹ s ⁻¹	10^2k_d , s ⁻¹	T , °C	$10^{-2}k_f$, M ⁻¹ s ⁻¹	10^2k_d , s ⁻¹
15.0	0.938	2.08	30.0	3.27	18.9
20.0	1.38	4.81	35.0	5.09	37.4
25.0	2.69	9.74			

^a $\mu = 0.10$ M (LiClO₄), pH = 8 (Tris).

The first-order rate constants obtained for the dissociation reactions were observed to be independent of the concentration of pyrazine (0.1–1 M) and were identified as the k_d for the reverse of reaction 1. The results are shown in column 3 of Table III. The low solubility of the tubercidin ligand introduced difficulty into the kinetic measurements, and its k_d was obtained from the intercept of the k_{obs} vs $[L]$ linear plot of the formation experiment. The rate constants of the dissociation, contrary to those of the formation, depend very much on the nature of the ligand, which, in turn, will affect the equilibrium constants in eq 1 (column 4 of Table III). The fast rates of dissociation of the adenosine, tubercidin, and 2-aminopyridine complexes in comparison with other aminopyridine complexes apparently arise from the steric hindrance, which turns out to be a more important factor than the contribution of π bonding in determining the stability of the complexes. The rate constants of dissociation for the 1-methyladenosine and 2-aminopyridine complexes can also be obtained from the intercepts of k_{obs} vs $[L]$ plots, and the results are close to the measured values, as shown in Table III. The low affinity of the 1-methyladenosine complex provides evidence that N-7 is not a likely binding site in the Fe(CN)₅sado³⁻ complex.

The temperature dependence of the rate constants of formation and dissociation were also studied for the Fe(CN)₅sado³⁻ complex, and the results are shown in Table IV. The plots of $\ln(k/T)$ vs $1/T$ are linear, as shown in Figure 3, yielding $\Delta H_f^\ddagger = 14.4 \pm 0.3$ kcal mol⁻¹, $\Delta S_f^\ddagger = 0.57 \pm 0.09$ cal deg⁻¹ mol⁻¹ and $\Delta H_d^\ddagger = 24.6 \pm 0.5$ kcal mol⁻¹, $\Delta S_d^\ddagger = 19.5 \pm 0.4$ cal deg⁻¹ mol⁻¹. The ΔH_f^\ddagger value is comparable with that of other pentacyanoferrate(II) systems,²⁰ indicating a common dissociative mechanism.

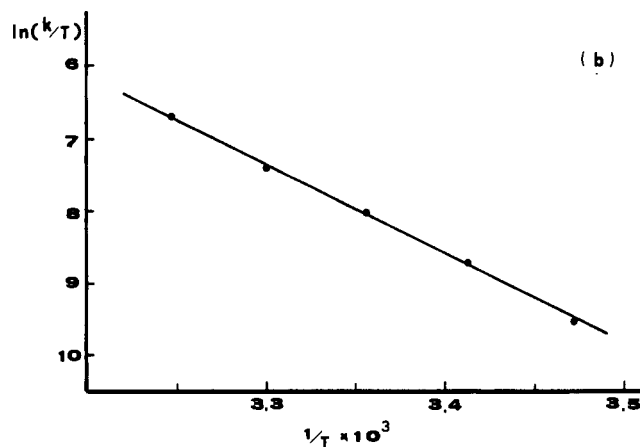
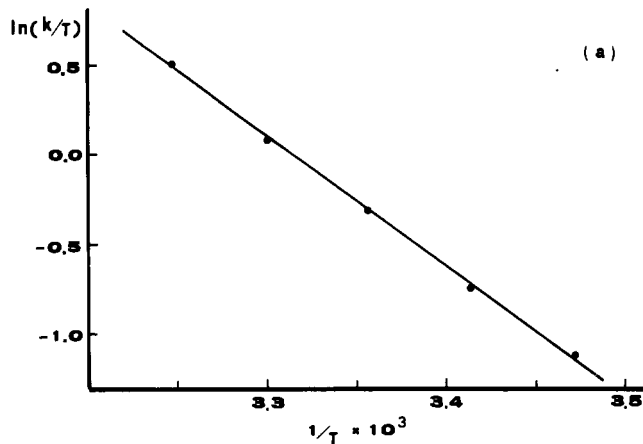


Figure 3. $\ln(k/T)$ vs $1/T$ plots for Fe(CN)₅sado³⁻ ($\mu = 0.10$ M (LiClO₄), pH = 8): (a) for rate constants of formation; (b) for rate constants of dissociation.

Table V. Reduction Potentials of the Fe(CN)₅L^{2-/3-} Complexes^a

L	$E_{1/2}$, V (vs NHE)	L	$E_{1/2}$, V (vs NHE)
adenosine	0.49	4-aminopyridine	0.33
1-methyladenosine	0.34		0.35 ^b
tubercidin	0.44	pyrimidine	0.52 ^c
2-aminopyridine	0.41	imidazole	0.35 ^d
3-aminopyridine	0.43		

^a $T = 25$ °C, $\mu = 0.10$ M (LiClO₄), pH = 8 (Tris). ^b Reference 15. ^c Reference 12. ^d Reference 22.

Electrochemistry. The reduction potentials for the various Fe(CN)₅L^{2-/3-} couples are shown in Table V. Potential measurements were made by cyclic voltammetry, and the reduction potentials of the complexes were taken at the midpoint between the anodic and cathodic peaks. The peak-to-peak separations of 60–80 mV indicate that the redox reactions belong to one-electron reversible processes. The reduction potential for the Fe(CN)₅sado^{2-/3-} couple of 0.49 V is close to the observed values for the tubercidin, 2-aminopyridine, and pyrimidine complexes, suggesting N-1 binding for the adenosine complex. The electrochemical results further confirm the spectroscopic prediction.

In the study of the adenosine complex of pentaammineruthenium, Clarke^{4,7} discovered a linkage isomerization from N-1 to the adjacent exocyclic amine nitrogen after the metal center is oxidized. The reverse movement also occurs when the Ru(III) complex is reduced back to the Ru(II) complex.⁷ One piece of the evidence for this isomerization reaction comes from the electrochemical results. The measured reduction potential of the solution of (adenosine)pentaammineruthenium(III) (–0.04 V vs NHE) is much less than might be expected for a N-1 bound isomer, which should be analogous to that of the corresponding

(21) Coelho, A. L.; Toma, H. E.; Malin, J. M. *Inorg. Chem.* 1983, 22, 2903.
 (22) Toma, H. E.; Creutz, C. *Inorg. Chem.* 1977, 16, 545.

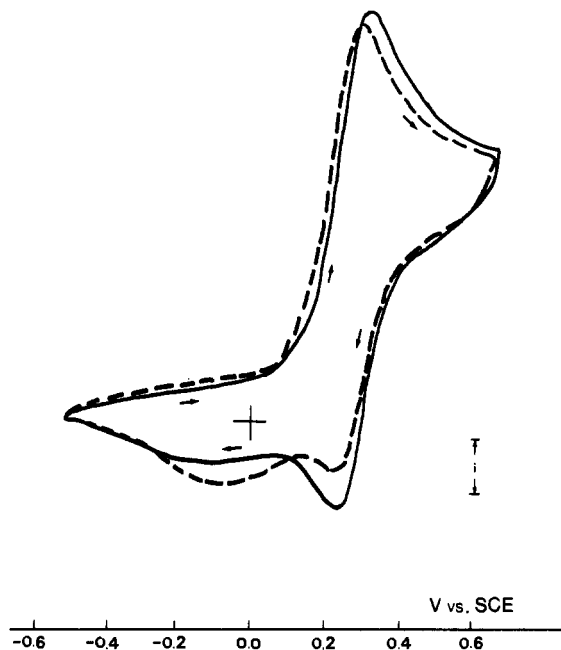
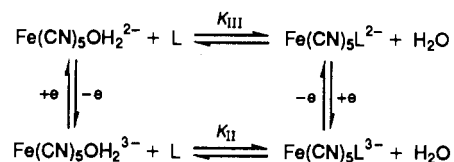


Figure 4. Cyclic voltammograms of the $[\text{Fe}(\text{CN})_5\text{ado}]^{2-/3-}$ couple (1.0×10^{-3} M, 25°C , 0.10 M LiClO_4): (—) measured in $\text{Fe}(\text{CN})_5\text{ado}^{3-}$ solution; (---) measured in $\text{Fe}(\text{CN})_5\text{ado}^{2-}$ solution.

pyrimidine (pyr) complex. The $E_{1/2}$ of the $\text{Ru}(\text{NH}_3)_5\text{pyr}^{3+/2+}$ couple has a value of 0.43 V.⁴ Further support for exocyclic nitrogen binding would be the similarity in the absorption patterns for the pentaammineruthenium(III) complexes of adenosine, 1-methyladenosine, and tubercidin. For the adenosine complex of pentacyanoferrate, the spectral results favored the N-1 coordination for both Fe(II) and Fe(III) metal centers, as we have mentioned earlier. The formal potential measurements for solutions of both the $\text{Fe}(\text{CN})_5\text{ado}^{3-}$ complex and its oxidized form yield the same value at 0.49 V, which is similar to that of the $\text{Fe}(\text{CN})_5\text{pyr}^{2-/3-}$ couple: 0.52 V. Moreover, the cyclic voltammograms for the solutions of both oxidation states are rather similar, as is shown in Figure 4. The bump at -0.07 V (vs SCE) on the reduction cycle may arise from the unreacted $\text{Fe}(\text{CN})_5\text{OH}_2^{2-/3-}$ species remaining in solution. Cyclic voltammetry of the $\text{Fe}(\text{CN})_5\text{OH}_2^{2-/3-}$ couple (at $\sim 1 \times 10^{-4}$ M) also shows an irreversible wave at -0.09 V (vs SCE) in the reduction cycle at $\text{pH} = 8$ and $\mu = 0.10$ M (LiClO_4). Obviously, the electrochemical results also indicate that both Fe(II) and Fe(III) in the adenosine complex coordinate at the same site and no linkage isomerization occurs upon oxidation. Facile linkage isomerization between different oxidation states of the metal center has been observed for a variety of pentaammineruthenium complexes with poly-

functional ligands.²³⁻²⁷ However, no such observation has ever been reported for the pentacyanoferrate system. One explanation may arise from the steric effect. If the linkage isomerization proceeds through a seven-coordinated transition state for the Ru(III) complexes,²⁵ a similar reaction could be prohibited due to the steric hindrance of the 3d metal ion for the pentacyanoferrate complexes. Another explanation, at least in the case of the adenosine complex, may be the lack of hydrogen-bonding stabilization for the exocyclic amine-bonded pentacyanoferrate(III) complex as is observed for the pentaammineruthenium(III) complex.⁴ In the adenosine complex of $\text{Ru}(\text{NH}_3)_5^{3+}$, which is coordinated through the exocyclic nitrogen, the N-1 on the pyrimidine ring can be hydrogen-bonded to the coordinated ammine hydrogen of Ru(III).

From the reduction potentials and the values of K_{II} , we can estimate the equilibrium constants for the formation of $\text{Fe}(\text{CN})_5\text{L}^{2-}$ complexes, K_{III} , by utilizing the following cycle and eq 2.²²



$$E^\circ(\text{Fe}(\text{CN})_5\text{L}^{2-/3-}) = E^\circ(\text{Fe}(\text{CN})_5\text{OH}_2^{2-/3-}) + \frac{RT}{F} \ln \frac{K_{\text{II}}}{K_{\text{III}}} \quad (2)$$

The values of K_{III} are listed in column 5 of Table III. It is noteworthy that when the nitrogen on the imidazole ring is the coordination site, the affinity of the complexes favors the Fe(III) state. Thus K_{III} is greater than K_{II} by ~ 5 -fold for the imidazole and ~ 7 -fold for the 1-methyladenosine complex. However, when N-1 is the site of coordination, the Fe(II) form is much favored and $K_{\text{II}}/K_{\text{III}}$ is ~ 49 for the adenosine and ~ 7 for the tubercidin complex. This implies that π back-bonding is much more important when coordination occurs at the six-membered ring. For the 4-aminopyridine complex, $K_{\text{III}} > K_{\text{II}}$ is expected because of the resonance of the amino lone pair, which will stabilize the π donation of Fe(III). The reverse is true for the 3-aminopyridine complex, where the resonance is minor.

Acknowledgment. Support of this work by the National Science Council of the Republic of China under Grant NSC74-0208-M033-01 is gratefully acknowledged.

(23) Diamond, S. E.; Taube, H. *J. Am. Chem. Soc.* **1975**, *97*, 5921.

(24) Yeh, A.; Taube, H. *J. Am. Chem. Soc.* **1980**, *102*, 4725.

(25) Yeh, A.; Scott, N.; Taube, H. *Inorg. Chem.* **1982**, *21*, 2542.

(26) Ilan, Y.; Taube, H. *Inorg. Chem.* **1983**, *22*, 3144.

(27) Fairlie, D. P.; Taube, H. *Inorg. Chem.* **1985**, *24*, 3199.